Journal of Power Sources 267 (2014) 14–19

Contents lists available at ScienceDirect

Journal of Power Sources

journal homepage: www.elsevier.com/locate/jpowsour

Fraction of the theoretical specific energy achieved on pack level for hypothetical battery chemistries

Damla Eroglu [a, b, *], Seungbum Ha [a, b], Kevin G. Gallagher [a, b]

[a] Joint Center for Energy Storage Research, Argonne National Laboratory, Argonne, IL, USA
[b] Chemical Sciences and Engineering Division, Argonne National Laboratory, Argonne, IL, USA

HIGHLIGHTS

- Fraction of the theoretical specific energy achieved on pack level is estimated.
- Fraction of the theoretical specific energy depends greatly on OCV, $\bar{E}_{theo}$ and ASI.
- Lower $\bar{E}_{theo}$ systems capture higher fraction of the theoretical specific energy.
- Pack-level properties are independent of $\bar{E}_{theo}$ in low OCV systems at moderate ASI.
- Reducing impedance in low OCV systems leads to higher pack-level specific energies.

ARTICLE INFO

Article history:
Received 13 February 2014
Received in revised form
21 April 2014
Accepted 8 May 2014
Available online 22 May 2014

Keywords:
Beyond lithium-ion
Lithium-ion
Battery design
System analysis
Specific energy
Energy density

ABSTRACT

In valuing new active materials chemistries for advanced batteries, the theoretical specific energy is commonly used to motivate research and development. A packaging factor is then used to relate the theoretical specific energy to the pack-level specific energy. As this factor is typically assumed constant, higher theoretical specific energies are judged to result in higher pack-level specific energies. To test this implicit assumption, we calculated the fraction of the theoretical specific energy achieved on the pack level for hypothetical cell chemistries with various open-circuit voltages and theoretical specific energies using a peer-review bottom-up battery design model. The pack-level specific energy shows significant dependence on the open-circuit voltage and electrochemical impedance due to changes in the quantity of inactive materials required. At low-valued average open-circuit voltages, systems with dramatically different theoretical specific energies may result in battery packs similar in mass and volume. The fraction of the theoretical specific energy achieved on the pack level is higher for the lower theoretical specific energy systems mainly because the active materials mass dominates the pack mass. Finally, low-valued area-specific impedance is shown to be critical for chemistries of high theoretical specific energy and low open-circuit voltage to achieve higher pack-level specific energies.

1. Introduction

New lithium-ion and beyond lithium-ion battery chemistries are being developed in the hopes of enabling cost-effective electric vehicles [1–17]. In the search for new candidates, the theoretical specific energy (i.e. W h kg^{-1}) is frequently used for the justification of research and development investment in particular chemistries. The theoretical specific energy, $\bar{E}_{theo}$, is calculated considering the mass of the active materials as shown in equation (1) [2–5,7]. However the pack-level specific energy, $\bar{E}_{pack}$, depends on the mass of the entire battery pack (i.e. active and inactive materials) [18]. The implicit assumption with the use of $\bar{E}_{theo}$ to value candidate materials is that the pack-level specific energy is a constant fraction of the theoretical value as shown in equation (2) [1,2,4,6,7]. Since these new chemistries are not yet commercialized, practical specific energies and energy densities are not available; system-level properties are predicted using the packaging factors for today's batteries. In the literature, values of 0.2–0.45 are commonly used for f_m [1,2,4,6,7].

$$\bar{E}_{theo} = \frac{C \cdot U_{Batt}}{(m_{ne,act} + m_{pe,act})} \quad (1)$$

* Corresponding author. Chemical Sciences and Engineering Division, Argonne National Laboratory, 9700 S Cass Avenue, Bldg. 200, Argonne, IL 60439-4854, USA. Tel.: +1 630 252 1974.
E-mail addresses: eroglud@anl.gov, damlaeroglu@gmail.com (D. Eroglu).

http://dx.doi.org/10.1016/j.jpowsour.2014.05.071
0378-7753/

$$\bar{E}_{pack} = \bar{E}_{theo} \cdot f_m \quad (2)$$

Here C is the cell capacity, U_{Batt} is the average battery open-circuit voltage (OCV), $m_{ne,act}$ and $m_{pe,act}$ are the mass of the active materials in the negative and positive electrode, respectively, and f_m is the fraction of the theoretical specific energy achieved on pack level.

Although the fraction of the theoretical specific energy is commonly used for pack-level estimations, there are no studies in the literature to our knowledge that investigates f_m as a function of the cell chemistry. The theoretical energy content of a material does not depend on the individual magnitude of the cell capacity or average voltage but rather the product of these two values, $C \cdot U_{Batt}$ (equation (1)). However, we will show that the resulting specific energy of the battery is more strongly dependent on the voltage when battery packs are designed at constant peak power efficiency. In this study, the peer reviewed, bottom-up Battery Performance and Cost (BatPaC) model [19,20] has been modified to systematically estimate the fraction of the theoretical specific energy and energy density achieved on pack level as a function of OCV and $\bar{E}_{theo}$. In other words, the objective of this work is to understand how the relative ratio of active to inactive materials changes within a battery pack as physicochemical properties of a material change, namely the voltage, specific capacity, and impedance. The need to remove energy from the battery at finite power levels directly affects the amount of inactive materials through changes in cell area and electrode thickness [18]. While comparison of the calculated values in this study with nonexistent commercially available battery packs is impossible, the trends that are demonstrated will hold true for the future chemistries that are currently under development in laboratories worldwide. Therefore, the value of this theoretical assessment is to highlight challenges that must be overcome through science and engineering advancements for materials that might initially appear to promise extremely high specific energy.

2. Model description

The BatPaC model (a detailed model description is available elsewhere [19,20]) is a publically available bottom-up design and cost model developed through support by the U.S. Department of Energy Vehicle Technologies Office. BatPaC was peer reviewed sponsored by the U.S. Environmental Protection Agency (EPA) [21] and used to assist the 2017–2025 light duty vehicle rule for fuel economy and greenhouse gas emissions in the United States [22].

The design methodology used in BatPaC has been previously validated against cylindrical wound cell formats [23]. The calculated materials quantities agreed with the actual values within 3%. Moving to the prismatic format now used in BatPaC simplifies the current collection calculation while leaving the governing equations unchanged. The performance calculation has also been improved by including additional physics in the impedance calculation. This approach has been validated against experimental measurements with a graphite/$LiNi_{0.8}Co_{0.15}Al_{0.05}O_2$ cell using electrodes up to 100 μm in thickness [24].

By bottom-up design model, we mean all necessary components required to produce DC electricity are sized and included in the pack-level values (e.g. current collectors, cell packaging, battery housing, and thermal management). Fig. 1 presents a schematic of the cell- and pack-level designs in the BatPaC model. The cell design is similar to those that exist in commercial products while the module and pack design reflect the expected improved packaging that will result from continued engineering improvements in product design. Thus the projected pack-level specific energy and energy density can be considered optimistic compared to values obtain in vehicles batteries used in model year 2013.

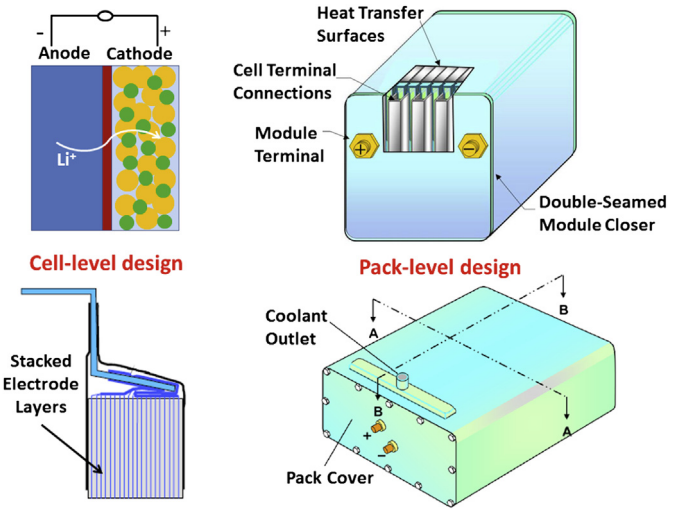

Fig. 1. Schematic of cell-level and pack-level designs in BatPaC.

The pack is designed for a 50 kW h, 100 kW and 360 V battery containing 50% excess lithium-metal (Li-metal) as the negative electrode. For the positive electrode, hypothetical OCVs and specific capacities required for batteries with $\bar{E}_{theo}$ of 500, 750, 1000, 1500 and 2000 W h kg^{-1} are considered. The specific capacity of the positive electrode at a given $\bar{E}_{theo}$ is calculated as a function of OCV using equation (3) (derived from equation (1)) and then fed into the modified BatPaC model with the other design parameters as shown in Table 1. The change in the number of cells in a battery pack with the OCV to keep the pack voltage constant at 360 ± 10 V is also taken into account in the model as shown in equation (4). The pack voltage is set by the powertrain electronics architecture and should not be battery chemistry specific, to the first order of analysis.

$$c_{pe} = \frac{1}{\left(\frac{U_{OCV}}{\bar{E}_{theo}} - \frac{[N/P]}{c_{ne}}\right)} \quad (3)$$

$$U_{Batt} = U_{OCV} \cdot N_{cell} \quad (4)$$

Here, c_{pe} is the specific capacity of the positive electrode and N_{cell} is the number of cells in a battery pack. The definitions of the other variables are given in Table 1.

Pack-level specific energy, energy density and the fractions of the theoretical values on the pack level are calculated using the modified BatPaC model for these hypothetical U_{OCV} and $\bar{E}_{theo}$ couples. For the material properties of the hypothetical cathodes, the experimentally measured properties of NMC441 ($Li_{1.05}(Ni_{4/9}Mn_{4/9}Co_{1/9})_{0.95}O_2$) in the BatPaC model is used [19,20,25]. The properties

Table 1
Parameters used in BatPaC for the pack design.

Parameter	Symbol	Value
Energy (kW h)	E	50
Rated power (kW)	P	100
Average battery open-circuit voltage (V)	U_{Batt}	360
Average cell open-circuit voltage (V)	U_{OCV}	1.5–4.5
Negative electrode specific capacity (mA h g^{-1})	c_{ne}	3860
Negative to positive capacity ratio	$[N/P]$	1.5
Theoretical specific energy (W h kg^{-1})	$\bar{E}_{theo}$	500–2000
Target voltage efficiency at rated power	$[V/U]$	0.8
Maximum electrode thickness limitation (μm)	$L_{pos,max}$	100
Area-specific impedance parameter (Ω cm^2)	ASI_{const}	33

of Li-metal are used for the negative electrode and the changes in thickness of the negative electrode are removed from the ASI calculation, reflection of the lack of porosity in the metal electrode. For the estimation of the slope of the OCV curve in the model, the difference between the average OCV for discharge (U_{OCV}, at 50% state-of-charge (SOC)), and OCV at full power ($U_{OCV,p}$, at 20% SOC) is taken as 250 mV based on the experimental data on NMC441 [25]. In the calculation of the system-level specific energy and energy density, the total energy content for the battery ($\Delta SOC = 100\%$) is considered rather than the energy required for a reduced operating SOC window of the battery.

3. Results and discussion

The pack-level specific energy predictions are shown in Fig. 2a as a function of OCV for various $\bar{E}_{theo}$. At low voltages, the effect of $\bar{E}_{theo}$ on the pack-level predictions is insignificant. However with increasing voltage, the pack-level specific energy continues to increase for the high $\bar{E}_{theo}$ whereas it reaches to a plateau for the lower values. This could be explained by the area of the positive electrode, A_{pos}, which dictates the area of the battery pack, A_{pack} by equation (7). The required cell area is set by the target voltage at rated power, $U_{OCV,p}$, and the area-specific impedance for power, ASI_p. The cell area decreases with increasing OCV (equation (5)) [20]. Since both cell area and number of cells decrease with increasing voltage, the pack area also decreases as shown in Fig. 2b. However at low theoretical specific energies, $\bar{E}_{theo}$, the maximum thickness limitation is reached at high voltages (Fig. 2b); the cell area is now dictated by the cell capacity requirement to achieve the energy demands of the battery as shown in equation (6) [20].

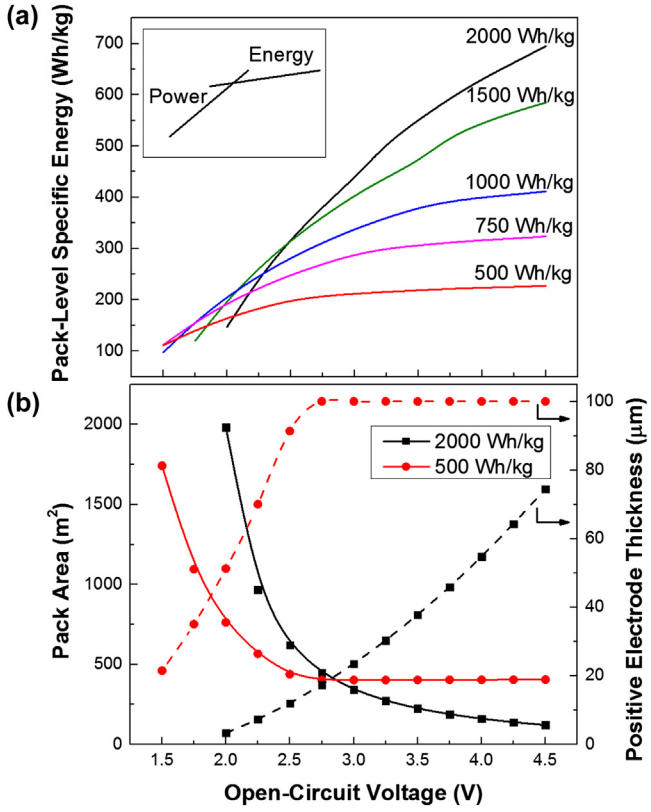

Fig. 2. The effect of average OCV on the (a) pack-level specific energy and (b) pack area and positive electrode thickness for different $\bar{E}_{theo}$. Two limiting behavior on the pack-level specific energy can be seen in (a): (1) area determined by power and (2) area determined by energy.

Maximum electrode thickness is a practical limitation set by the battery performance and life considerations which may be adversely affected by nonuniform current distribution, repeated volume expansion, side reactions, or poor cold-temperature performance [20]. When the thickness limitation is reached, the cell area starts to increase with increasing voltage preventing the pack area from decreasing any further (Fig. 2b). The difference between U_{OCV} and $U_{OCV,p}$ is assumed as 250 mV as mentioned in the previous section. The choice of this value does not affect the general conclusions discussed above but shifts the point where the energy to power trend change is seen in Fig. 2a.

$$A_{pos} = \frac{P \cdot ASI_p}{N_{cell} \cdot U_{OCV,p}^2 \cdot \left[\frac{V}{U}\right] \cdot \left(1 - \left[\frac{V}{U}\right]\right)} \tag{5}$$

$$A_{pos} = \frac{C}{L_{pos,max} \cdot c_{pe}} \tag{6}$$

$$A_{pack} = N_{cell} \cdot A_{pos} \tag{7}$$

The use of BatPaC for the projection of detailed mass and volume breakdowns is necessary. However the complexity of the model may seem to complicate the analysis of this behavior. The observed behavior in Fig. 2 may also be understood through use of equation (5) alone to compare two different cell chemistries with the same theoretical specific energy. A detailed discussion on cell and pack area as a function of average cell OCV using equation (5) can be found in the Appendix.

It is apparent from Fig. 2a that for chemistries with low OCV, the advantage of high $\bar{E}_{theo}$ cannot be utilized at this impedance level. This could be explained by the dependence of the mass of inactive materials (carbon and binder in the electrode, electrolyte, separator, current collectors, and packaging) and its ratio to the active materials on OCV as shown in Fig. 3 for the highest and lowest theoretical specific energy cases. It can be seen that the inactive materials mass is significantly higher at low OCVs especially for high theoretical specific energies. Simply put, while the mass of the active materials remains nearly invariant as determined by $\bar{E}_{theo}$, the mass of the inactive materials is driven by the power requirements (equation (5)) and thus changes considerably. As a result, the ratio of the active to inactive materials mass increases with OCV. Another important conclusion is

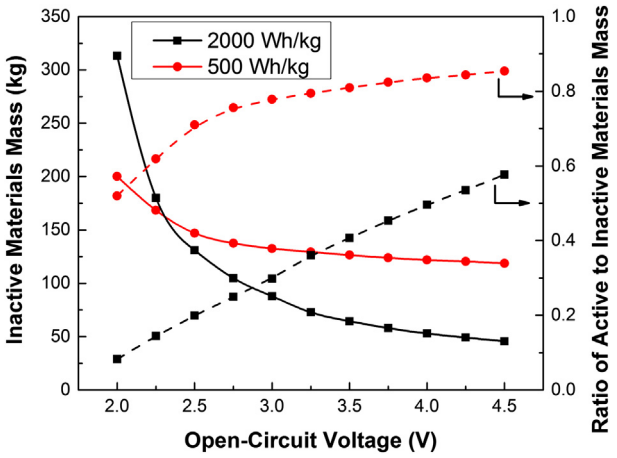

Fig. 3. The effect of average OCV on inactive materials mass and ratio of active to inactive materials mass for theoretical specific energies of 500 and 2000 W h kg^{-1}.

that the inactive materials mass and its ratio to the active materials are greatly different for the low and high specific energy systems.

In order to have a better understanding of this significant dependence of the inactive materials mass on OCV, mass and volume breakdown of the pack is presented in Fig. 4 for a theoretical specific energy of 750 W h kg^{-1}. It can be seen that at low OCVs and moderate impedances the pack suffers from high packaging and current collector mass penalty due to very thin electrodes and large cell area. As the maximum thickness limitation is reached at increasing OCVs, the decrease in the mass of the cell components (current collectors, electrolyte and separator) with OCV ends, preventing the pack mass to decrease any further.

When the volume breakdown is investigated for the same pack (Fig. 4b), it is seen that the current collectors do not show any dominance at low OCVs unlike Fig. 4a mainly because of the low thickness of these components within the cell. The main contributors of the pack volume besides packaging are the active materials and electrolyte (active material and separator volume in the figure do not include the void volume; the electrolyte filling the void space in the porous electrode and separator is shown separately). At higher OCVs, the active materials and packaging volume continue to decrease whereas the volume of all the other cell components stays constant. It is apparent from Fig. 4 that mass and volume breakdown of the pack is critical in understanding the trends of the pack mass and volume as a function of OCV and theoretical specific energy.

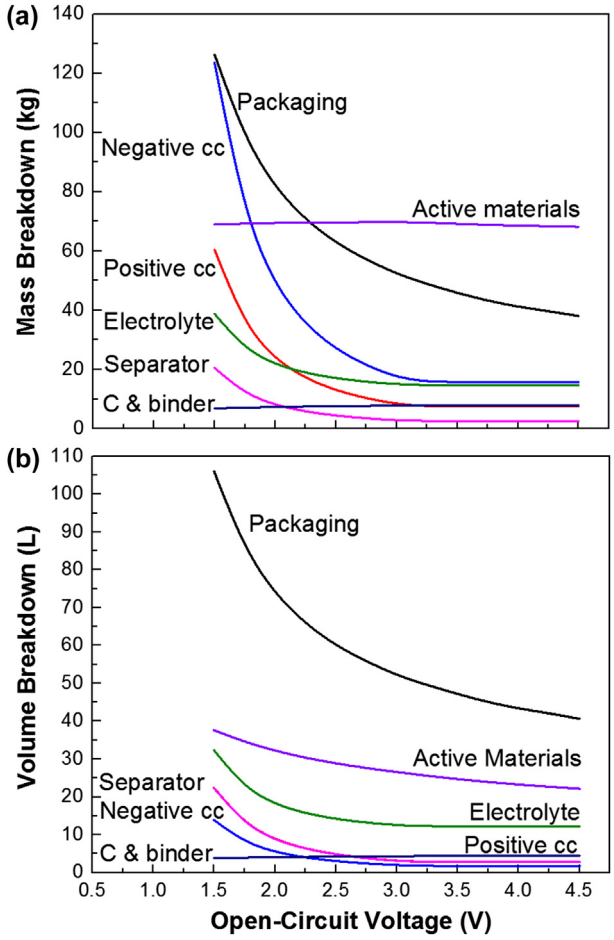

Fig. 4. The effect of average OCV on (a) mass and (b) volume breakdown of the pack ($\bar{E}_{theo}$ = 750 W h kg^{-1}).

The fraction of the theoretical specific energy achieved on the pack level, f_m, as a function of OCV and $\bar{E}_{theo}$ can be seen in Fig. 5. The trends for the high and low $\bar{E}_{theo}$ curves are as discussed in Fig. 2a. The interesting result in Fig. 5 is that systems with lower $\bar{E}_{theo}$ capture higher fractions of the theoretical specific energy on the pack level. This could be explained by the definition of f_m, which can be simplified into the ratio of the active materials mass to pack mass in equation (2). As also evident from Fig. 4a, for low or moderate theoretical specific energy chemistries, the active materials mass is dominant; it presents a higher percentage of the pack mass thus higher f_m. Consequently, materials with a high $\bar{E}_{theo}$ should be expected, to the first order estimation, to have a higher relative packing burden than materials with lower $\bar{E}_{theo}$.

The fraction of the theoretical energy density achieved on the pack level, f_v, varies less significantly with $\bar{E}_{theo}$ and OCV compared to f_m as presented in Fig. 5 inset. In order to understand this weaker dependence of f_v on $\bar{E}_{theo}$ and OCV, the mass, volume and density of the active materials as a function of the average OCV are compared for the high and low theoretical specific energy cases as shown in Fig. 6. The total active materials mass remains unchanged at constant $\bar{E}_{theo}$ as shown in Fig. 6 and expected from equation (1). However, the ratio of positive electrode to negative electrode mass, consequently the active material density, increases significantly with decreasing $\bar{E}_{theo}$ or increasing OCV (Fig. 6). As a result of the active material density change, the ratio of the active material volume to pack volume, hence f_v, becomes less sensitive to $\bar{E}_{theo}$ or OCV. The dramatically different densities of the assumed lithium metal negative electrode and metal oxide positive electrode drive this behavior (i.e. 0.5 vs 4.6 g cm^{-3}).

Finally, the effect of area-specific impedance on the pack-level specific energy is investigated for $\bar{E}_{theo}$ of 2000 W h kg^{-1} as shown in Fig. 7. The ASI is a combination of all the transport and charge transfer resistances in the cell components and their interfaces [20,24]. In the model, one of the components of the total system ASI is a constant based on experimental data, ASI_{const}, which is approximated as invariant with the thickness of the positive electrode [20,24]. All the previous results were discussed for moderate impedances (i.e. ASI_{const} = 33 Ω cm^2). In order to study the effect of ASI without losing the dependence on the electrode thickness, ASI_{cons} is changed between 5 and 30 Ω cm^2. It can be seen in Fig. 7 that at high OCVs, the ASI has only a modest effect on the pack-level specific energy. Conversely, decreasing the ASI for cells with low OCVs results in a significant increase in the pack-level predictions. This is demonstrated by systems with lower ASI

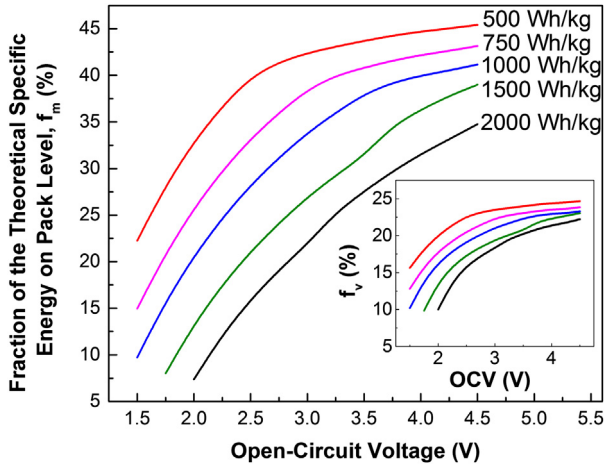

Fig. 5. The effect of average OCV on the fraction of the theoretical specific energy and (inset) energy density on pack level for different $\bar{E}_{theo}$.

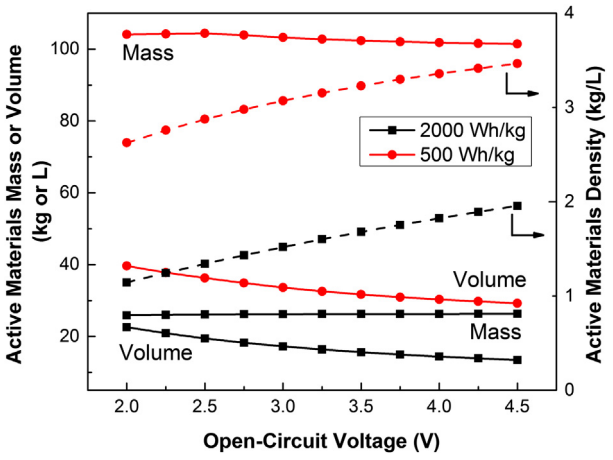

Fig. 6. The effect of average OCV on the mass, volume and density of the active materials for theoretical specific energies of 500 and 2000 W h kg^{-1}.

reaching the maximum thickness limitation at increasing voltages (Fig. 7 inset).

An important challenge is understood from this materials-to-systems analysis regarding capturing the highest fraction of a material's theoretical energy storage capability. For electrochemical couples with low OCV and high $\bar{E}_{theo}$, the ASI is a critical parameter that must be considered as fundamental as the voltage and specific capacity of the cell couple. Various means exist for lowering the cell impedance, though most, if-not-all, result in a trade-off to lower packaging factors, f_m. Materials level performance improvements may come from advances in controlling particle size and morphology [26]. Conversely, systems level approaches to increasing material performance may require operating at elevated temperature thus creating additional mass, volume, and efficiency burdens. This analysis is especially important for not yet commercialized chemistries like Li–S ($\bar{E}_{theo}$ = 2567 W h kg^{-1} and OCV = 2.2 V vs Li) and multivalents to show that estimating system-level properties using theoretical predictions is not straight forward for these low average OCV systems.

This analysis can be extended for Li-ion chemistries as shown Fig. 8. Similar trends are seen for the pack-level specific energy as a

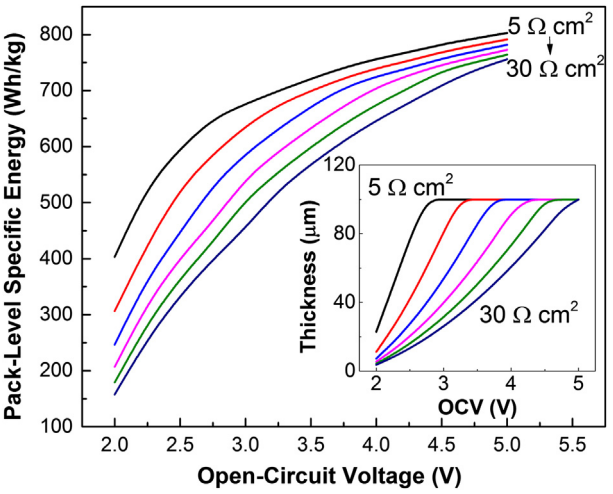

Fig. 7. The effect of cell ASI on the pack-level specific energy and (inset) positive electrode thickness as a function of average OCV ($\bar{E}_{theo}$ = 2000 W h kg^{-1}).

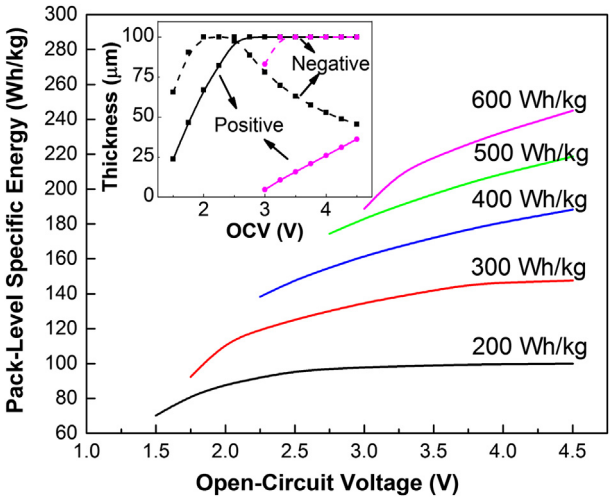

Fig. 8. The extended analysis for Li-ion chemistries (Li metal anode is replaced with graphite in the model) showing the effect of average OCV on the pack-level specific energy and (inset) positive (solid) and negative (dashed) electrode thickness for $\bar{E}_{theo}$ of 200 W h kg^{-1} (black squares) and 600 W h kg^{-1} (pink circles) (For interpretation of the references to color in this figure legend, the reader is referred to the web version of this article.).

function of OCV and $\bar{E}_{theo}$ (Fig. 2a vs Fig. 8). At low theoretical specific energies, the maximum electrode thickness limitation is reached at the positive electrode preventing the pack-level specific energy to increase any further (Fig. 8 inset). However at higher theoretical specific energies, the negative electrode thickness becomes limiting (Fig. 8 inlet). The discussions presented previously for f_m and f_v can also be extended for the Li-ion chemistries. However it should be emphasized that in the analysis, low and high theoretical specific energies for beyond Li-ion and Li-ion chemistries span different ranges (i.e., 200–600 W h kg^{-1} vs 500–2000 W h kg^{-1}) due to the dramatically different specific capacities of graphite (330 mA h g^{-1}) and Li metal (3860 mA h g^{-1}).

The analysis presented in this work provides a framework for explaining the dependence of the pack-level properties on the cell chemistry and impedance. The trends presented can be used when evaluating a range of potential material chemistries for research and development efforts for electric drive vehicle batteries. To fully understand one particular chemistry, a detailed material-to-system analysis must be undertaken utilizing experimentally determined constraints and material properties. For instance, the electrode thickness limitations are poorly understood and may vary for different chemistries. In addition, ASI calculations may be dissimilar for different chemistries displaying significant non-linearity not captured here.

4. Conclusions

The specific energies achieved at the pack level for batteries are significantly different than the theoretical values determined from molecular masses and the free energy of the reaction. The fraction of the theoretical specific energy on pack level depends greatly on the OCV, $\bar{E}_{theo}$, and ASI. The OCV of the system is found to be critical. Pack-level specific energies do not benefit from high theoretical values at low OCVs and moderate impedances. To obtain higher pack-level specific energies for systems with low OCV, the ASI of the system should be reduced. The presented study is significant in providing a framework to estimate the pack-level specific energies of new chemistries using their open-circuit voltage and theoretical predictions.

Acknowledgments

This work was supported as part of the Joint Center for Energy Storage Research, an Energy Innovation Hub funded by the U.S. Department of Energy, Office of Science, Basic Energy Sciences. The submitted manuscript has been created by UChicago Argonne, LLC, Operator of Argonne National Laboratory ("Argonne"). Argonne, an U.S. Department of Energy Office of Science laboratory, is operated under Contract No. DE-AC02-06CH11357.

Appendix. Dependence of the cell and pack area on the average OCV of the cell

In order to show the dependence of the cell and pack area on the average open-circuit voltage more clearly, the area calculations for two packs with equal energy and power requirements and pack voltages (50 kW h, 100 kW and 360 V) are compared in this section. Using equation (5), the ratio of the cell area of pack 1 ($U_{OCV} = 2$ V) to pack 2 ($U_{OCV} = 4$ V) can be written as in equation (A1). As described previously in the main text, the open-circuit voltage at rated power, $U_{OCV,p}$, is assumed to be 0.25 V less than the average open-circuit voltage of the cell. In addition, N_{cell} changes as a function of open-circuit voltage to keep the pack voltage constant; therefore $N_{cell,2V}$ is twice that of $N_{cell,4V}$. Finally assuming the ASI_p of the two chemistries are the same, the ratio of the cell area of two packs can be calculated as:

$$\frac{A_{pos,2V}}{A_{pos,4V}} = \frac{N_{cell,4V}}{N_{cell,2V}} \cdot \left(\frac{U_{OCV,p,4V}}{U_{OCV,p,2V}}\right)^2 = \frac{1}{2} \cdot \left(\frac{3.75\ \text{V}}{1.75\ \text{V}}\right)^2 = 2.3 \qquad \text{(A1)}$$

Translating the cell area into pack area by equation (7), the ratio of the pack areas can be calculated as in equation (A2).

$$\frac{A_{pack,2V}}{A_{pack,4V}} = \left(\frac{U_{OCV,p,4V}}{U_{OCV,p,2V}}\right)^2 = \left(\frac{3.75\ \text{V}}{1.75\ \text{V}}\right)^2 = 4.6 \qquad \text{(A2)}$$

This sample calculation shows the critical dependence of pack-level properties on the average cell open-circuit voltage; a 2 V chemistry must have more than 4 times bigger area to achieve the same pack energy, power and voltage requirements as a 4 V chemistry with the same theoretical specific energy.

References

[1] G. Girishkumar, B. McCloskey, A.C. Luntz, S. Swanson, W. Wilcke, J. Phys. Chem. Lett. 1 (2010) 2193–2203.
[2] M.M. Thackeray, C. Wolverton, E.D. Isaacs, Energy Environ. Sci. 5 (2012) 7854–7863.
[3] J. Christensen, P. Albertus, R.S. Sanchez-Carrera, T. Lohmann, B. Kozinsky, R. Liedtke, J. Ahmed, A. Kojic, J. Electrochem. Soc. 159 (2012) R1–R30.
[4] P.G. Bruce, S.A. Freunberger, L.J. Hardwick, J.-M. Tarascon, Nat. Mater. 11 (2012) 19–29.
[5] M. Barghamadi, A. Kapoor, C. Wen, J. Electrochem. Soc. 160 (2013) A1256–A1263.
[6] V.S. Kolosnitsyn, E.V. Karaseva, Russ. J. Electrochem.+ 44 (2008) 506–509.
[7] P.G. Bruce, L.J. Hardwick, K. Abraham, MRS Bull. 36 (2011) 506–512.
[8] M.R. Palacin, Chem. Soc. Rev. 38 (2009) 2565–2575.
[9] K.M. Abraham, Z. Jiang, J. Electrochem. Soc. 143 (1996) 1–5.
[10] D. Aurbach, Z. Lu, A. Schechter, Y. Gofer, H. Gizbar, R. Turgeman, Y. Cohen, M. Moshkovich, E. Levi, Nature 407 (2000) 724–727.
[11] D. Aurbach, G.S. Suresh, E. Levi, A. Mitelman, O. Mizrahi, O. Chusid, M. Brunelli, Adv. Mater. 19 (2007) 4260–4267.
[12] J.-P. Gabano, Lithium Batteries, Academic Press, London and New York, 1983.
[13] E. Peled, Y. Sternberg, A. Gorenshtein, Y. Lavi, J. Electrochem. Soc. 136 (1989) 1621–1625.
[14] R. Rauh, K. Abraham, G. Pearson, J. Surprenant, S. Brummer, J. Electrochem. Soc. 126 (1979) 523–527.
[15] H. Yamin, E. Peled, J. Power Sources 9 (1983) 281–287.
[16] S.-E. Cheon, K.-S. Ko, J.-H. Cho, S.-W. Kim, E.-Y. Chin, H.-T. Kim, J. Electrochem. Soc. 150 (2003) A800–A805.
[17] J. Auborn, Y. Barberio, J. Electrochem. Soc. 132 (1985) 598–601.
[18] K.G. Gallagher, S. Goebel, T. Greszler, M. Mathias, W. Oelerich, D. Eroglu, V. Srinivasan, Energy Environ. Sci. 7 (2014) 1555–1563.
[19] P.A. Nelson, K.G. Gallagher, I. Bloom, BatPaC (Battery Performance and Cost) Software, 2012.
[20] P. Nelson, K. Gallagher, I. Bloom, D. Dees, Modeling the Performance and Cost of Lithium-ion Batteries for Electric Vehicles, Chemical Sciences and Engineering Division, Argonne National Laboratory, Argonne, IL USA, 2011. ANL-11/32.
[21] Peer Review Report for the ANL BatPaC Model: Modeling the Cost and Performance of Lithium-ion Batteries for Electric-drive Vehicles, 2011 docket ID EPA-HQ-OAR-2010-0799-1080.
[22] Joint Technical Support Document: Final Rulemaking for 2017-2025 Light-duty Vehicle Greenhouse Gas Emission Standards and Corporate Average Fuel Economy Standards, United States Environmental Protection Agency, 2012. EPA-420-R-12-901.
[23] P. Nelson, I. Bloom, K. Amine, G. Henriksen, J. Power Sources 110 (2002) 437–444.
[24] K.G. Gallagher, P.A. Nelson, D.W. Dees, J. Power Sources 196 (2011) 2289–2297.
[25] S.H. Kang, W.Q. Lu, K.G. Gallagher, S.H. Park, V.G. Pol, J. Electrochem. Soc. 158 (2011) A936–A941.
[26] A.S. Arico, P. Bruce, B. Scrosati, J.M. Tarascon, W. Van Schalkwijk, Nat. Mater. 4 (2005) 366–377.